Absence of a reductase, NCB5OR, causes insulin-deficient diabetes

Jianxin Xie*, Hao Zhu*, Kevin Larade*, Annie Ladoux*†, Ayden Seguritan*, Michelle Chu*, Susumu Ito‡, Roderick T. Bronson§, Edward H. Leiter¶, Chen-Yu Zhang‖, Evan D. Rosen‖, and H. Franklin Bunn*,**

*Hematology Division, Brigham and Women's Hospital, ‖Division of Endocrinology, Beth Israel Deaconess Medical Center, and Departments of ‡Cell Biology and §Pathology, Harvard Medical School, Boston, MA 02115; and ¶The Jackson Laboratory, Bar Harbor, ME 04609

Communicated by Donald F. Steiner, University of Chicago, Chicago, IL, June 7, 2004 (received for review May 3, 2004)

NCB5OR is a highly conserved NAD(P)H reductase that contains a cytochrome b5-like domain at the N terminus and a cytochrome b5 reductase-like domain at the C terminus. The enzyme is located in the endoplasmic reticulum (ER) and is widely expressed in organs and tissues. Targeted inactivation of this gene in mice has no impact on embryonic or fetal viability. At 4 weeks of age, *Ncb5or*−/− mice have normal blood glucose levels but impaired glucose tolerance. Isolated *Ncb5or*−/− islets have markedly impaired glucose- or arginine-stimulated insulin secretion. By 7 weeks of age, these mice develop severe hyperglycemia with markedly decreased serum insulin levels and nearly normal insulin tolerance. As the animals age, there is a progressive loss of beta cells in pancreatic islets, but there is no loss of alpha, delta, or PP cells. Electron microscopy reveals degranulation of beta cells and hypertrophic and hyperplastic mitochondria, some of which contain electron dense inclusions. Four-week-old *Ncb5or*−/− mice have enhanced sensitivity to the diabetogenic agent streptozotocin. NCB5OR appears to play a critical role in protecting pancreatic beta cells against oxidant stress.

Impaired insulin production and secretion is central to the pathogenesis of diabetes mellitus. In type 1 diabetes, affected individuals experience autoimmune destruction of beta cells within pancreatic islets that leads to a marked reduction in insulin production. In type 2, the more prevalent form of diabetes, patients have insulin resistance in skeletal muscle, fat, and liver, and develop a relative impairment of insulin production in beta cells. Both disorders are polygenic. Genome-wide scans have uncovered multiple loci in humans and mice that impact susceptibility to both type 1 (1–3) and type 2 (4, 5) diabetes. However, only a few of these contributory genes have been identified. Although monogenic causes of diabetes are much less common, they offer unique insights into genes that are important in insulin production and glucose homeostasis. Maturity onset diabetes in the young (MODY) is an autosomal dominant disorder caused by mutations either in glucokinase, which significantly contributes to the sensing of glucose within beta cells (6), or in several transcription factors known to play critical roles in beta cell function (7, 8). Other single gene defects that cause human diabetes include mutations in mitochondrial genes (9–11) as well as genes encoding insulin and insulin receptor (4).

Monogenic mouse models of diabetes have provided additional independent information on genes that regulate insulin production. The vital contribution of the endoplasmic reticulum (ER) to beta cell viability and function is demonstrated by two informative mutations. PERK, a kinase located in the ER, contributes to the ability of that organelle to adapt to the accumulation of unfolded proteins (12, 13). *Perk*−/− mice develop insulin-deficient diabetes because of impairment of the beta cell's response to ER stress (14, 15). The Akita mouse is a naturally occurring maturity onset diabetes in the young (MODY) model in which a C96Y mutation in insulin 2 causes heterozygous mice to have diabetes (16). The ER in the beta cells of Akita mice are dysfunctional because of accumulation of proinsulin that cannot fold properly due to its inability to form one of its critical disulfide bonds. In this report, we describe the diabetic phenotype of mice having targeted inactivation of *Ncb5or*, which encodes a highly conserved, ubiquitously expressed and soluble flavoheme NAD(P)H reductase (17) that is localized in the ER (18).

Materials and Methods

Generation of *Ncb5or* Knockout Mice. The mouse *Ncb5or* genomic DNA fragments were cloned by screening the 129Sv genomic library built in bacterial artificial chromosome vectors (Research Genetics, Huntsville, AL). A targeting vector was constructed by replacing the DNA region, from 3′ end of intron 3 to the 5′ end of intron 4, including the entire exon 4, with a *Pgk-Hyg* expression cassette. The genomic DNA in this vector included a 5.6-kb 5′ flank and a 3.2-kb 3′ flank. After being linearized, the targeting vector was electroporated into 129SvS4Jae embryonic stem (ES) cells. After hygromycin selection, heterozygous *Ncb5or* knockout ES clones were identified by Southern blot hybridization. Four targeted clones were injected into blastocysts obtained from BALB/cAnN mice (Taconic Farms). The chimeric embryos were then implanted into the uteri of pseudopregnant mice, and the pups, upon maturation, were bred with BALB/cAnN mice. Germ-line transmission of the offspring was analyzed by Southern blot hybridization as well as by PCR. Gender-matched *Ncb5or* +/+ and −/− littermates from breedings of the F_2 *Ncb5or* +/− mice were used in all of the experiments.

The animal experimentation protocol pertaining to this work was approved by Harvard Medical Area Standing Committee on Animals. Mice were handled in accordance with the guidelines issued by the National Institutes of Health. The animals used in this study were housed in a pathogen-free facility on a 12-h light/dark cycle with ad libitum access to food and water.

mRNA Analysis. Northern blot analysis was performed on total RNAs extracted from various tissues by TRIzol reagent (Invitrogen). The randomly labeled 415-nt probe is from a region between the exon 4/exon 5 boundary and exon 11 and was PCR amplified by 5′ primer, 5′-GAAGCCTGCTGTTCCAAAAGACTGTCATGAAGGA-3′, and 3′ primer, 5′-CATGTTTCTCCAGGTGATCACCAAGACATTGCC-3′. Access RT-PCR System (Promega) was used to detect *Ncb5or* mRNA species by using 5′ primer, 5′-ATGGATTGGATCCGACTGACC-3′, an oligonucleotide from exon 2, and 3′ primer, 5′-GCAGTGTGTCTGACATTTGGCT-3′, which is from exon 6.

Western Blotting. Total homogenates were prepared from pancreata of *Ncb5or* +/+ and −/− mice. Equal amount of protein

Abbreviations: ER, endoplasmic reticulum; ROS, reactive oxygen species; STZ streptozotoccin.

†Present address: Centre National de la Recherche Scientifique, Unité Mixte de Recherche 6543, Centre de Biochimie, Parc Valrose, 06108 Nice Cedex 2, France.

**To whom correspondence should be addressed. E-mail: hfbunn@rics.bwh.harvard.edu.

www.pnas.org/cgi/doi/10.1073/pnas.0404044101

was loaded onto 8% and 10% SDS polyacrylamide gel. SeeBlue Plus2 (Invitrogen) was used as the protein standard. Western blot analysis was performed by using rabbit polyclonal antibody against full-length mouse NCB5OR diluted 1/1,000 (Genemed Synthesis) as the primary antibody, and anti-rabbit IgG diluted 1/1,500 (Cell Signaling) was used as the secondary antibody. Bands were visualized with enhanced chemiluminescence system (Pierce).

Blood Glucose, Serum Insulin, Glucose and Insulin Tolerance Tests, and Streptozotocin (STZ) Sensitivity Experiments. Blood samples from fed animals were collected between 8 a.m. to noon. For glucose tolerance tests, mice were fasted overnight for 14 h followed by i.p. injection of glucose (2 mg/g body weight, except for the mice in STZ sensitivity experiment, which received 1 mg/g body weight). Blood samples were obtained from tail veins at 0, 15, 30, 60, 90, and 120 min after injection, and the glucose levels were assessed by using a glucometer (One Touch, Lifescan). For insulin tolerance tests, mice were fasted for 6 h followed by i.p. injection of recombinant human insulin (1 unit/kg body weight, Eli Lily). Serum insulin concentrations were assayed by using a mouse insulin ELISA kit (Crystal Chem) and a mouse insulin standard.

Four-week-old female *Ncb5or* +/+ and −/− mice were i.p. injected with STZ (Sigma, 10 mg/kg body weight per day) for 4 days, followed by an injection of 50 mg/kg body weight, before measurement of blood glucose levels at the fed state for 5 days. Four-week-old male *Ncb5or* +/+ and −/− mice were challenged by i.p. injection of STZ (10 mg/kg body weight per day) for 4 days before subjecting them to a glucose tolerance test. Sodium citrate buffer (0.1 M, pH 4.6) was used to inject the mice of the same age and gender in the control groups.

Immunohistochemistry. Mice were killed by CO_2 asphyxiation, and the pancreata were fixed in 4% neutrally buffered paraformaldehyde at room temperature overnight and embedded in paraffin. Insulin and glucagon were detected on the 5-μm pancreatic sections by guinea pig anti-human insulin diluted 1/100 (Linco) and rabbit anti-glucagon diluted 1/3,000 (a kind gift from Susan Bonner–Weir), respectively, followed by incubation with peroxidase-conjugated AffiniPure goat anti-rabbit Ig (H+L) diluted 1/1,000 (Jackson ImmunoResearch). 3,3-diaminobenzidine tetrahydrochloride (DAB) was applied to the sections as the substrate for peroxidase. The sections were counterstained by hematoxylin.

Transmission Electron Microscopy. After vascular perfusion of the whole mouse via intracardiac puncture with 2.5% glutaraldehyde and 2% paraformaldehyde in 0.1 M sodium cacodylate buffer (pH 7.4), the pancreata were stored in dilute fixative. They were sliced (0.5 mm thick), placed in aqueous 1% osmium tetroxide and 1.5% potassium ferrocyanide for 1 h at room temperature, and washed with water and 0.5 M maleate buffer (pH 5.2). The tissues were then treated with 1% uranyl acetate in maleate buffer and washed in water. After dehydration with graded cold ethanol, the sections were embedded in Epon or Epon Araldite. Thin sections were placed on bare grids and stained in saturated uranyl acetate diluted with equal parts of acetone. After lead citrate staining, the sections were examined and photographed with a JEOL 1200 EX electron microscope.

Studies on Isolated Islets. To isolate islets, the hepatopancreatic ampulla was clamped and Liberase RI (Roche Diagnostics) was injected through the common bile duct into the pancreatic duct to perfuse the pancreas. After digestion at 37°C for 25 min, washing, and centrifugation on a discontinuous Ficoll gradient (11, 21, 23, and 25%), pancreatic islets were harvested from the 11–21% interface. Islets were cultured for 20–24 h in RPMI medium 1640 (BioWhittaker) with 5.5 mM glucose, 7.5% FBS (GIBCO/BRL), and 1% penicillin–streptomycin (GIBCO/BRL). For insulin secretion experiments, three islets were transferred to individual Eppendorf tubes containing DMEM (ICN Biochemicals) with 5.5 mM glucose, 25 mM glucose, or 20 mM L-arginine/25 mM glucose and 0.1% gelatin (Difco) and incubated at 37°C for 1 h. Insulin concentrations in the supernatants were determined by ELISA assays. For evaluation of the total insulin content, 15 islets were transferred to each tube containing DMEM with 5.5 mM glucose at 37°C for 1 h. Islets were pelleted, homogenized, and sonicated, and the supernatants were assayed for insulin.

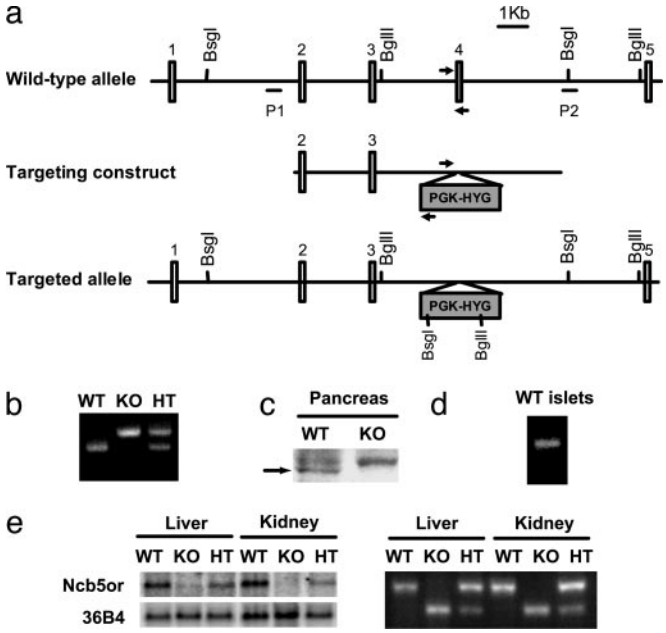

Fig. 1. Generation of *Ncb5or* −/− mice. (*a*) Schematic representation of the *Ncb5or* wild-type allele, knockout targeting construct and targeted allele. The *Bsg*I and *Bgl*II sites and P1 and P2 probes were used to genotype the mice by Southern blots. The arrows represent the primers used in genotyping by PCR. (*b*) Genotyping of mice by multiplex PCR. The primers for wild-type allele (WT) amplify a 366-bp product, and the primers for knockout allele (KO) amplify a 427-bp product. (*c*) Western blot analysis of NCB5OR protein (arrow) in pancreata. The upper band represents a nonspecific protein. (*d*) RT-PCR analysis of expression of *Ncb5or* mRNA in isolated islets of *Ncb5or* +/+ mice. (*e*) Northern blot (*Left*) and RT-PCR (*Right*) analyses of *Ncb5or* mRNA in livers and kidneys of *Ncb5or* +/+ (WT), −/− (KO), and +/− (HT) mice. The mRNA detected in the +/+ mice was derived from the wild-type allele. The mRNA detected in −/− mice was derived from the knockout allele, which lacks the entire exon 4.

Results

Generation of *Ncb5or* Knockout Mice. In the targeting vector, the genomic region encoding the exon 4 of *Ncb5or* gene was replaced by a hygromycin resistance cassette (Fig. 1*a*). This exon contains the heme-binding domain of NCB5OR, which has been shown to be crucial for both its enzyme stability and biochemical properties (19). Approximately 25% of the offspring of *Ncb5or* +/− parents were null (−/−) homozygotes. Thus, absence of the *Ncb5or* gene had no detectable impact on embryonic or fetal viability.

The homozygous knockout mice do not express full-length *Ncb5or* mRNA (Fig. 1*e*) and NCB5OR protein (Fig. 1*c*) in any of the tissues tested. A minute amount of mRNA was detected in these homozygotes (Fig. 1*e*). This mRNA species was derived from the knockout allele and lacked the entire exon 4 (Fig. 1*e*). If translated, it would encode a short polypeptide of 123 amino

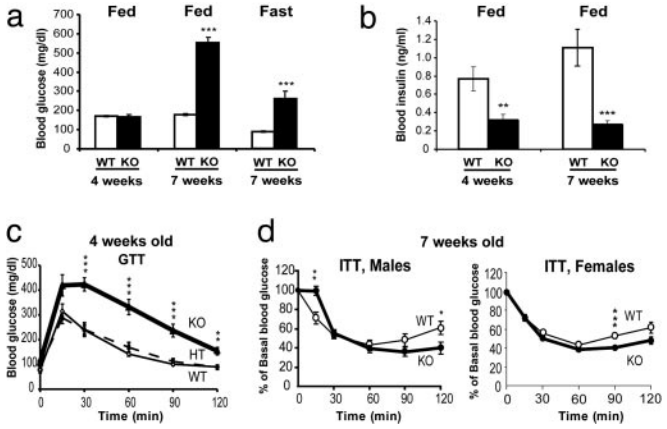

Fig. 2. Metabolic measurements in *Ncb5or* +/+, +/−, and −/− mice. (*a*) Blood glucose levels in fed male mice of age 4 weeks (*n*: WT = 7, KO = 7) and fed or fasting male mice of age 7 weeks (*n*: WT = 8, KO = 9). (*b*) Serum insulin levels in fed male mice of age 4 weeks (*n*: WT = 6, KO = 7) and fed male mice of age 7 weeks (*n*: WT = 8, KO = 9). (*c*) Glucose tolerance tests (GTT) on *Ncb5or* +/+ (WT), +/− (HT), and −/− (KO) male mice of age 4 weeks (*n*: WT = 8, HT = 12, KO = 7). (*d*) Insulin tolerance tests (ITT) on 7-week-old male (*Left*, *n*: WT = 8, KO = 8) and female (*Right*, *n*: WT = 10, KO = 12) mice. Error bars designate mean ± SEM. *, $P < 0.05$; **, $P < 0.01$; ***, $P < 0.001$ versus WT, unpaired two-tailed *t* test.

acid residues unlikely to fold into a stable functional protein due to the lack of NCB5OR sequence downstream of exon 3. Western blots of knockout tissues were probed with polyclonal antibodies against NCB5OR holoprotein or the N-terminal 15 residues, and no such species were detected (data not shown).

The phenotype of *Ncb5or* −/− animals was studied in three genetic backgrounds: C57BL/6;129, BALB/cAnN;129, and pure 129. All of the results presented below pertain to animals with a BALB/cAnN;129 mixed genetic background. However, the identical diabetic phenotype has also been seen in *Ncb5or* −/− C57BL/6;129 and *Ncb5or* −/− 129 animals. None of the knockout mice had any abnormalities either on gross or microscopic examination except for the pancreatic islet histopathology described below, food intake, and body fat. Compared with +/+ mice, *Ncb5or* −/− mice have increased food intake and decreased mass of adipose tissue (see supporting information, which is published on the PNAS web site). A wide range of routine hematology and chemistry tests on *Ncb5or* −/− mice uncovered no abnormalities except those pertaining to diabetes described below and hyperlipidemia (see supporting information). Thus, the *Ncb5or* −/− animals have a rather pure diabetic/fat phenotype. In contrast, *Ncb5or* +/− heterozygotes have normal blood sugar levels, glucose tolerance (Fig. 2*c*), serum lipid profiles, and mass of white adipose tissue (data not shown).

Glucose Homeostasis in *Ncb5or*−/− Mice. ***Transition from prediabetic to diabetic phenotype.*** To evaluate the effect of *Ncb5or* knockout on glucose homeostasis, we examined blood glucose and serum insulin levels in wild-type (+/+) and homozygous *Ncb5or* knockout (−/−) littermates. All of the results shown are on male mice, unless stated otherwise. Female *Ncb5or* −/− mice have a diabetic phenotype indistinguishable from that of males. At 4 weeks of age, in the fed state, *Ncb5or* −/− mice had normal blood glucose levels (Fig. 2*a*) but insulin levels were 40% those of wild-type littermates (Fig. 2*b*). These animals had impaired tolerance to an i.p. injection of glucose (Fig. 2*c*), suggesting decreased insulin reserve, i.e., prediabetes. By 7 weeks of age, the blood glucose levels in *Ncb5or* −/− mice were 3-fold higher than those in +/+ mice during the fed state or after an overnight fast (Fig. 2*a*). The hyperglycemia in the *Ncb5or* −/− animals was associated with a marked reduction in plasma insulin. In the fed state, insulin levels of 7-week-old *Ncb5or* −/− animals were decreased to 25% of the levels in normal animals (Fig. 2*b*). Insulin was barely detectable in the plasma of fasting *Ncb5or* −/− animals (data not shown). These data indicate that, between 4 and 7 weeks of age, there was a progressive deterioration of glucose homeostasis in *Ncb5or* −/− mice.

Loss of pancreatic beta cells. The marked hyperglycemia in *Ncb5or* −/− mice could be due to a combination of decreased insulin production or secretion, as suggested by low insulin levels (Fig. 2*b*) and insulin resistance, similar to human type 2 diabetes. However, these animals had nearly normal insulin tolerance with slightly enhanced sensitivity (Fig. 2*d*); therefore, the diabetes phenotype cannot be explained by insulin resistance. Thus, a defect in the pancreatic beta cell appears to be responsible for dysregulated glucose homeostasis in *Ncb5or* −/− mice. To pursue this question, we assessed pancreatic islet histology and *in situ* immunohistochemistry on sections from *Ncb5or* +/+ and −/− mice of 4, 7, and 21 weeks of age. In the older *Ncb5or* −/− mice, hematoxylin and eosin-stained sections revealed a modest but significant reduction in the number of islets and a decrease in the cytoplasmic to nuclear ratio of islet cells. However, no infiltration of inflammatory cells was noted in any of the specimens, and no phagocytosis of necrotic beta cell fragments was observed. The latter phenotype has been commonly observed in monogenic obesity models producing beta cell-specific loss and islet atrophy, such as the C57BLKS-*Lepr*^{db} (*db*/*db*) mouse (20, 21). As shown in Fig. 3*A*, immunostaining with antibodies against insulin and glucagon revealed cell distribution patterns in 4-week-old *Ncb5or* −/− islets that were nearly indistinguishable from +/+ islets. At this age, a large mass of insulin-producing beta cells was surrounded by a thin peripheral layer of glucagon-producing alpha cells. Immunostaining with an antibody specific for proinsulin (a kind gift of Ole D. Madsen) revealed no difference between islets of *Ncb5or* −/− and +/+ mice. At 7 weeks, *Ncb5or* −/− mice exhibited a striking decrease in the number of positively stained beta cells. Viability of other non-beta islet endocrine cells was unaffected, with islet cores now containing primarily alpha cells. The loss of beta cells in *Ncb5or* −/− mice progressed over time. At 21 weeks, only a very small number of stainable beta cells remained in pancreatic islets, and alpha cells were distributed throughout the islet. The localization of delta and PP cells was similar to that of alpha cells (data not shown). The beta cells that remained in the *Ncb5or* −/− sections of all three age groups consistently displayed less intensity than the wild-type controls, suggesting decreased insulin content. The progression of beta cell loss over time coincided with development of overt diabetes in *Ncb5or* −/− mice.

We found no evidence for enhanced apoptosis in *Ncb5or* −/− islets. Terminal deoxynucleotidyltransferase-mediated dUTP nick end labeling (TUNEL) staining on islets of 2- and 4-week-old animals showed no significant difference between *Ncb5or* −/− and +/+ mice (data not shown). There was also no evidence on either light or electron microscopy of enhanced apoptosis in *Ncb5or* −/− islets. Moreover, lack of any difference in the expression of Ki-67 protein suggested that inactivation of *Ncb5or* had no significant effect on cell proliferation in islets (data not shown). The fact that we have been unable to document enhanced apoptosis may be due to small differences in the rate of cell death extended over a period of several weeks. In addition, apoptotic cells are quickly cleared by the immune system *in vivo* (22).

Fig. 3*Ba* illustrates the ultrastructural features of a typical islet from 7-week-old wild-type male mice. Well granulated beta cells were the predominant endocrine cell class. In contrast, islets from diabetic *Ncb5or* −/− males were markedly depleted of

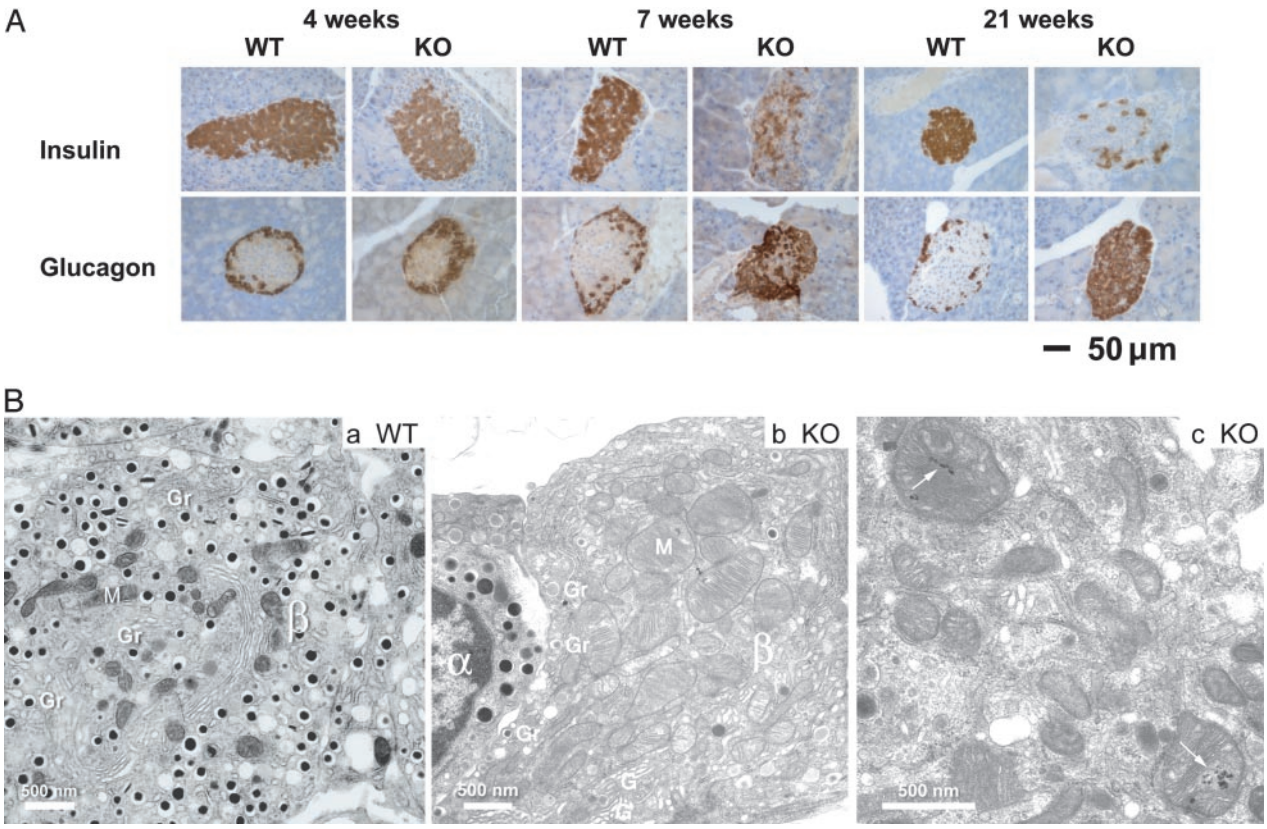

Fig. 3. Immunohistochemical and ultrastructural assessment of insulin- and glucagon-producing cells. (*A*) Pancreatic sections from *Ncb5or* +/+ and −/− male mice of 4, 7, and 21 weeks of age were stained *in situ* by using anti-insulin antibody for beta cells and anti-glucagon antibody for alpha cells. The immunostains are shown in brown color. (*B*) Electron micrographs from 7-week-old male *Ncb5or* +/+ and −/− mice. (*a*) In *Ncb5or* +/+ islets, well granulated beta cells (β) are the predominant islet cell type. Alpha cells (α) are less numerous. (*b*) Dearth of beta cells (β) in an *Ncb5or* −/− islet. The beta cell in the field is heavily degranulated. Mitochondria (M) are increased in number and in size. Golgi stacks (G) are prominent, but β granules (Gr) are reduced in number and primarily associated with the plasma membrane (emiocytosis). (*c*) Electron-dense inclusions (arrows) are present within some mitochondria in an islet from the same *Ncb5or* −/− mouse shown in *b*.

beta cells, producing an increased volume density of the alpha, delta, and PP cell classes. The residual beta cells present in islets of *Ncb5or* −/− mice were markedly degranulated (Fig. 3*Bb*), with the insulin-containing β granules mostly at the cell periphery (compare Fig. 3*B a* and *b*). This combination of reduced granule content and granule margination was indicative of hypersecretory activity. An unusual feature of these surviving beta cells was an increase in both the number and size of mitochondrial profiles (Fig. 3*Bb*). As shown in Fig. 3*Bc*, electron-dense inclusions were detected in some of these beta cells. No pathologic changes were detected in the non-beta endocrine cells in the atrophic islets, or in the exocrine or ductal epithelial cells in pancreata of *Ncb5or* −/− mice at any of the sampling points. Hence, the beta cells were selectively affected by the disruption of the *Ncb5or* gene.

Studies on Isolated Islets. The loss of beta cells explains the overt diabetes in *Ncb5or* −/− mice beyond 7 weeks of age. However, it cannot account for the prediabetic glucose intolerance seen in 4-week-old *Ncb5or* −/− mice. The deficiency in the acute response to external glucose challenge, together with the normal fed- and fasting-state blood glucose levels, indicates defective insulin release in response to glucose. To further address this issue, we assayed glucose-stimulated insulin secretion *in vitro* on size-matched isolated islets from 4-week-old *Ncb5or* +/+ and −/− mice. The insulin secretion rate in *Ncb5or* −/− islets was reduced by 62% and 87% with 5.5 mM glucose and 25 mM glucose inductions, respectively (Fig. 4*a*). These results provide evidence for an early defect in glucose-stimulated insulin secretion from the pancreatic beta cell in *Ncb5or* −/− mice, preceding beta cell loss and onset of clinical diabetes.

Arginine induces insulin release by the beta cell via direct triggering of K^+ efflux and Ca^{2+} influx, thereby bypassing the glucose-sensing mechanism. To determine whether the insulin secretion defect is caused by impaired glucose sensing, we

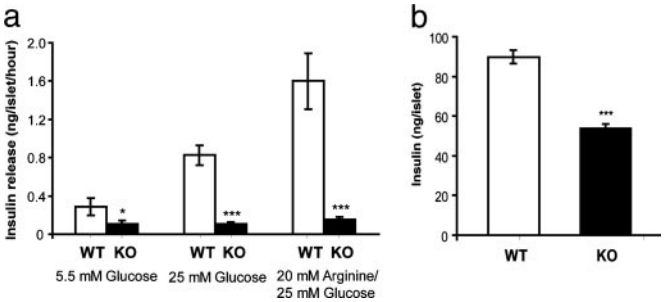

Fig. 4. Insulin release rate and total insulin content from isolated pancreatic islets. (*a*) Pancreatic islets were isolated from 4-week-old *Ncb5or* +/+ and −/− mice. After overnight incubation, the islets were treated with culture media containing 5.5 mM glucose, 25 mM glucose, or 20 mM L-arginine/25 mM glucose. Insulin released was then measured (*n*: WT = 8 and KO = 7–8). (*b*) Total insulin contents in isolated islets from 4-week-old *Ncb5or* +/+ and −/− mice. (*n*: WT = 7 and KO = 7). Error bars designate mean ± SEM. *, $P < 0.05$; **, $P < 0.01$; ***, $P < 0.001$ versus WT, unpaired two-tailed *t* test.

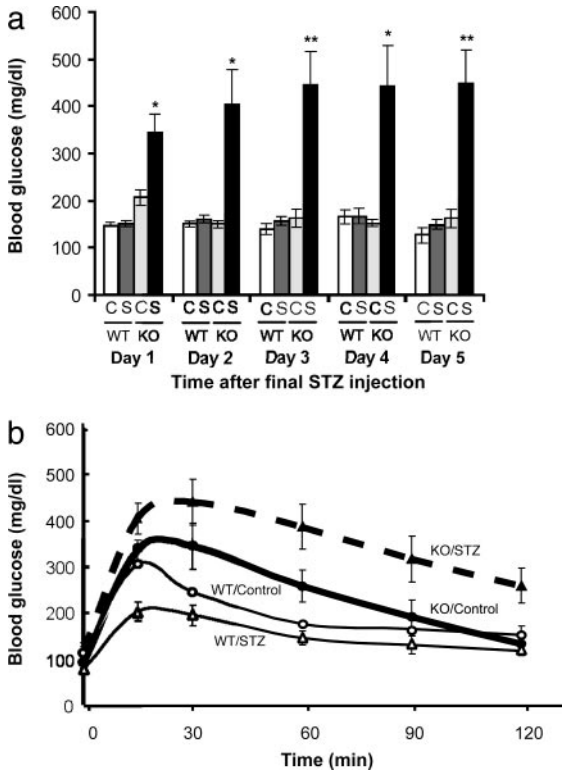

Fig. 5. Sensitivity of 5-week-old *Ncb5or* +/+ and −/− mice to STZ. (*a*) Fed blood glucose levels of STZ-treated (S) and untreated (C) female *Ncb5or* +/+ and −/− mice over 5 days after the final injection of the drug (*n*: STZ-treated WT = 5, untreated WT = 4, STZ-treated KO = 5, untreated KO = 4). Error bars designate mean ± SEM. *, $P < 0.05$; **, $P < 0.01$ versus untreated *Ncb5or*−/− mice, unpaired two-tailed *t* test. (*b*) Glucose tolerance test (1 mg of glucose per g of body weight, i.p.) on STZ-treated and untreated male *Ncb5or* +/+ and −/− mice (*n*: STZ-treated WT = 3, untreated WT = 2, STZ-treated KO = 5, untreated KO = 4). Error bars designate mean ± SEM.

analyzed the insulin release in response to L-arginine. With 20 mM L-arginine/25 mM glucose stimulation, insulin release rate on *Ncb5or* −/− islets dropped by 91% (Fig. 4*a*), a level similar to that seen under glucose stimulation. Thus, the insulin secretory defect in the 4-week-old mice is unlikely to be in the glucose-sensing pathway.

Previous *in situ* immunostaining results on the 4-week-old *Ncb5or* −/− pancreata suggested a decrease in total insulin content. Quantitative analysis of the total insulin contents showed a 40% decrease in 4-week-old *Ncb5or* −/− islets compared to size-matched +/+ islets (Fig. 4*b*). However, the suppression of insulin secretion in *Ncb5or* −/− islets greatly exceeded the reduction in insulin content (Fig. 4). This finding implies that, in these young *Ncb5or* −/− mice, impaired insulin secretion, rather than decreased biosynthesis, is the earliest beta cell defect.

Sensitivity to STZ. As shown in Fig. 5, 5-week-old *Ncb5or* −/− mice are unusually sensitive to the diabetogenic agent STZ. Untreated *Ncb5or* −/− animals had nearly normal fed blood glucose levels, whereas those treated with STZ had 70%, 168%, 175%, 191%, and 177% elevations over the 5 days after the final injection of the drug (Fig. 5*a*). STZ administration also resulted in an increased impairment of glucose tolerance in *Ncb5or* −/− mice (Fig. 5*b*). In contrast, the same dose schedules of STZ had no effect on fed blood glucose levels or glucose tolerance in *Ncb5or* +/+ mice (Fig. 5).

Discussion

Although *Ncb5or* is expressed in a broad range of animals and cells (17), including pancreata and islet cells (Fig. 1 *c* and *d*), the phenotype of the knockout mouse indicates that the critical biological role of this reductase is maintenance of viability of pancreatic beta cells. It is likely that this enzyme impacts importantly on the redox status of these cells. Beta cells in rodents are particularly susceptible to oxidant stress, perhaps owing to their unusually low expression of antioxidant enzymes such as catalase, glutathione peroxidase, as well as Mn and Cu/Zn superoxide dismutases (23–26). There is considerable, albeit indirect, evidence that, in type 1 diabetes, reactive oxygen species (ROS) cooperate with cytokines in the destruction of beta cells (27, 28). ROS also appear to play an important pathogenetic role in the gradual impairment of beta cell function in type 2 diabetes. Hyperglycemia per se results in marked up-regulation of antioxidant enzymes heme oxygenase-1 and glutathione peroxidase along with modest inductions of Cu/Zn and Mn superoxide dysmutases (29). Despite this adaptation, prolonged exposure to elevated glucose levels causes not only impaired insulin responsiveness, but also beta cell loss, due to ROS (30) arising from mitochondria (31, 32) and nonenzymatic glycation (33–35). This damage can be substantially prevented by the *in vivo* administration of antioxidants (36–38).

The selective toxicity of the well known diabetogenic agent STZ is likely due to the unusual vulnerability of the beta cell to oxidant stress. STZ generates hydrogen peroxide and induces DNA oxidation and fragmentation (39). STZ markedly affects intracellular redox status, lowering levels of reduced glutathione in pancreatic (40) and other (41) cells. The diabetogenic and redox effects of STZ can be reversed by the administration of the antioxidant nicotinamide (42–44). Our finding that *Ncb5or* −/− mice are particularly sensitive to STZ suggests that this flavoheme reductase plays an important role in protecting the pancreatic beta cell against oxidant stress.

An important clue to NCB5OR's biological function is its subcellular location. Both confocal microscopy and subcellular fractionation show that the protein is localized primarily in the endoplasmic reticulum (ER) (18). Regulated production of insulin in the beta cell puts an unusually heavy burden on the ER. Thus, if the stress response pathway is impaired, beta cells become dysfunctional and prematurely undergo apoptosis. It is noteworthy that the phenotype of the *Ncb5or* −/− mouse bears striking resemblance to that of two mouse models of ER stress in the beta cell, the Akita mouse (Ins2 C96Y) (16, 45) and the *Perk* knockout mouse (14, 15). All three have normal pancreatic and beta cell development, but at age 4–6 weeks develop progressive loss of beta cell mass and insulin-deficient diabetes. In view of the localization of NCB5OR in the ER, we hypothesize that this enzyme plays an intrinsic and critical role in the ER stress response pathway.

The beta cell's enhanced vulnerability to ER stress is likely due in part to superoxide generated by the formation of insulin's three disulfide bonds (13, 46, 47). It has been estimated that, in an average cell, ≈25% of its endogenous superoxide production arises from disulfide bond formation in the ER (46). In beta cells, the ER contribution to superoxide generation is likely to be higher. Because NCB5OR is a reducing enzyme localized in the ER, it may function to protect the cell from excess buildup of ROS.

In the beta cells of *Ncb5or* −/− mice, the mitochondria are hypertrophied and hyperplastic. It is likely that these mitochondrial abnormalities are a downstream response to ER stress. When the organelle's load of unfolded protein exceeds a critical threshold, a complex set of signaling pathways transduces responses into the mitochondria that trigger apoptosis. It is interesting that the phenotypes of three diabetic mouse models

of ER dysfunction (Akita, *Perk* −/−, and *Ncb5or* −/−) bear a striking resemblance to those of diabetic mice with beta cell conditional knockout of two mitochondrial proteins, Tfam (48) and frataxin (49). Within weeks after birth, all five of these mice develop glucose intolerance, hypoinsulinemia, and impaired glucose-induced insulin release from islets, followed by progressive loss of beta cells with a relative increase in alpha cells.

To understand the biological function of NCB5OR and its essential role in insulin production, it is necessary to identify its physiologic substrate(s) and product(s) and learn more about how this redox reaction impacts the unfolded protein pathway in the ER. Inquiry into NCB5OR's biological role should extend beyond the pancreatic beta cell. The widespread expression of this enzyme and its presence in lower organisms suggest that it may play a more general role in the ER stress response.

Drs. Susan Bonner-Weir and Mark Fleming provided helpful advice. Elizabeth Benecchi provided assistance in EM studies. This work was supported by National Institutes of Health Grants RO1 DK 56050 (to H.F.B.) and K01 DK59901 (to H.Z.), an Innovative Grant from the Juvenile Diabetes Research Foundation (to H.F.B.), and by National Sciences and Engineering Research Council (Canada) (K.L.) and Institut National de la Santé et de la Recherche Medicale (A.L.).

1. Todd, J. A. (1995) *Proc. Natl. Acad. Sci. USA* **92,** 8560–8565.
2. Concannon, P., Gogolin-Ewens, K. J., Hinds, D. A., Wapelhorst, B., Morrison, V. A., Stirling, B., Mitra, M., Farmer, J., Williams, S. R., Cox, N. J., *et al.* (1998) *Nat. Genet.* **19,** 292–296.
3. Atkinson, M. A. & Leiter, E. H. (1999) *Nat. Med.* **5,** 601–604.
4. Kahn, C. R., Vicent, D. & Doria, A. (1996) *Annu. Rev. Med.* **47,** 509–531.
5. Leiter, E. H. (1989) *FASEB J.* **3,** 2231–2241.
6. Matschinsky, F. M. (1996) *Diabetes* **45,** 223–241.
7. Fajans, S. S., Bell, G. I. & Polonsky, K. S. (2001) *N. Engl. J. Med.* **345,** 971–980.
8. Velho, G. & Robert, J. J. (2002) *Horm. Res.* **57,** 29–33.
9. Ballinger, S. W., Shoffner, J. M., Hedaya, E. V., Trounce, I., Polak, M. A., Koontz, D. A. & Wallace, D. C. (1992) *Nat. Genet.* **1,** 11–15.
10. van den Ouweland, J. M., Lemkes, H. H., Ruitenbeek, W., Sandkuijl, L. A., de Vijlder, M. F., Struyvenberg, P. A., van de Kamp, J. J. & Maassen, J. A. (1992) *Nat. Genet.* **1,** 368–371.
11. Reardon, W., Ross, R. J., Sweeney, M. G., Luxon, L. M., Pembrey, M. E., Harding, A. E. & Trembath, R. C. (1992) *Lancet* **340,** 1376–1379.
12. Harding, H. P., Zhang, Y. & Ron, D. (1999) *Nature* **397,** 271–274.
13. Harding, H. P., Zhang, Y., Zeng, H., Novoa, I., Lu, P. D., Calfon, M., Sadri, N., Yun, C., Popko, B., Paules, R., *et al.* (2003) *Mol. Cell* **11,** 619–633.
14. Harding, H. P., Zeng, H., Zhang, Y., Jungries, R., Chung, P., Plesken, H., Sabatini, D. D. & Ron, D. (2001) *Mol. Cell* **7,** 1153–1163.
15. Zhang, P., McGrath, B., Li, S., Frank, A., Zambito, F., Reinert, J., Gannon, M., Ma, K., McNaughton, K. & Cavener, D. R. (2002) *Mol. Cell. Biol.* **22,** 3864–3874.
16. Wang, J., Takeuchi, T., Tanaka, S., Kubo, S. K., Kayo, T., Lu, D., Takata, K., Koizumi, A. & Izumi, T. (1999) *J. Clin. Invest.* **103,** 27–37.
17. Zhu, H., Qiu, H., Yoon, H. W., Huang, S. & Bunn, H. F. (1999) *Proc. Natl. Acad. Sci. USA* **96,** 14742–14747.
18. Zhu, H., Larade, K., Jackson, T. A., Xie, J., Ladoux, A., Acker, H., Berchner-Pfannschmidt, U., Fandrey, J., Cross, A. R., Rodgers, K. R. & Bunn, H. F. (2004) *J. Biol. Chem.*, in press.
19. Davis, C. A., Dhawan, I. K., Johnson, M. K. & Barber, M. J. (2002) *Arch. Biochem. Biophys.* **400,** 63–75.
20. Like, A. A. (1985) in *The Diabetic Pancreas*, eds. Volk, B. W. & Arguille, E. R. (Plenum, New York), pp. 385–413.
21. Like, A. A. & Chick, W. L. (1970) *Diabetologia* **6,** 216–242.
22. Johnson, J. D., Ahmed, N. T., Luciani, D. S., Han, Z., Tran, H., Fujita, J., Misler, S., Edlund, H. & Polonsky, K. S. (2003) *J. Clin. Invest.* **111,** 1147–1160.
23. Grankvist, K., Marklund, S. L. & Taljedal, I. B. (1981) *Biochem. J.* **199,** 393–398.
24. Gandy, S. E., III, Galbraith, R. A., Crouch, R. K., Buse, M. G. & Galbraith, G. M. (1981) *N. Engl. J. Med.* **304,** 1547–1548.
25. Lenzen, S., Drinkgern, J. & Tiedge, M. (1996) *Free Radical Biol. Med.* **20,** 463–466.
26. Tiedge, M., Lortz, S., Drinkgern, J. & Lenzen, S. (1997) *Diabetes* **46,** 1733–1742.
27. Hanafusa, T. & Tarui, S. (1990) *Curr. Top. Microbiol. Immunol.* **156,** 15–25.
28. Mandrup-Poulson, T., Helqvist, S., Wogensen, L. D., Molvig, J., Pociot, F., Johanneson, J. & Nerup, J. (1990) *Curr. Top. Microbiol. Immunol.* **164,** 169–193.
29. Laybutt, D. R., Kaneto, H., Hasenkamp, W., Grey, S., Jonas, J. C., Sgroi, D. C., Groff, A., Ferran, C., Bonner-Weir, S., Sharma, A. & Weir, G. C. (2002) *Diabetes* **51,** 413–423.
30. Ihara, Y., Toyokuni, S., Uchida, K., Odaka, H., Tanaka, T., Ikeda, H., Hiai, H., Seino, Y. & Yamada, Y. (1999) *Diabetes* **48,** 927–932.
31. Nishikawa, T., Edelstein, D., Du, X. L., Yamagishi, S., Matsumura, T., Kaneda, Y., Yorek, M. A., Beebe, D., Oates, P. J., Hammes, H. P., *et al.* (2000) *Nature* **404,** 787–790.
32. Sakai, K., Matsumoto, K., Nishikawa, T., Suefuji, M., Nakamaru, K., Hirashima, Y., Kawashima, J., Shirotani, T., Ichinose, K., Brownlee, M. & Araki, E. (2003) *Biochem. Biophys. Res. Commun.* **300,** 216–222.
33. Baynes, J. W. (1991) *Diabetes* **40,** 405–412.
34. Kaneto, H., Fujii, J., Myint, T., Miyazawa, N., Islam, K. N., Kawasaki, Y., Suzuki, K., Nakamura, M., Tatsumi, H., Yamasaki, Y. & Taniguchi, N. (1996) *Biochem. J.* **320,** 855–863.
35. Matsuoka, T., Kajimoto, Y., Watada, H., Kaneto, H., Kishimoto, M., Umayahara, Y., Fujitani, Y., Kamada, T., Kawamori, R. & Yamasaki, Y. (1997) *J. Clin. Invest.* **99,** 144–150.
36. Kaneto, H., Kajimoto, Y., Miyagawa, J., Matsuoka, T., Fujitani, Y., Umayahara, Y., Hanafusa, T., Matsuzawa, Y., Yamasaki, Y. & Hori, M. (1999) *Diabetes* **48,** 2398–2406.
37. Tanaka, Y., Gleason, C. E., Tran, P. O., Harmon, J. S. & Robertson, R. P. (1999) *Proc. Natl. Acad. Sci. USA* **96,** 10857–10862.
38. Ihara, Y., Yamada, Y., Toyokuni, S., Miyawaki, K., Ban, N., Adachi, T., Kuroe, A., Iwakura, T., Kubota, A., Hiai, H. & Seino, Y. (2000) *FEBS Lett.* **473,** 24–26.
39. Takasu, N., Komiya, I., Asawa, T., Nagasawa, Y. & Yamada, T. (1991) *Diabetes* **40,** 1141–1145.
40. Kretowski, A., Szelachowska, M., Gorska, M., Zendzian-Piotrowska, M., Wysocka-Solowie, B. & Kinalska, I. (1996) *Horm. Metab. Res.* **28,** 35–36.
41. Slonim, A. E., Fletcher, T., Burke, V. & Burr, I. M. (1976) *Diabetes* **25,** 216–222.
42. Dulin, W. E. & Wyse, B. M. (1969) *Proc. Soc. Exp. Biol. Med.* **130,** 992–994.
43. Wright, J. R., Jr., Mendola, J. & Lacy, P. E. (1988) *Experientia* **44,** 38–40.
44. Rasschaert, J., Ling, Z. & Malaisse, W. J. (1993) *Mol. Cell Biochem.* **120,** 135–140.
45. Yoshioka, M., Kayo, T., Ikeda, T. & Koizumi, A. (1997) *Diabetes* **46,** 887–894.
46. Tu, B. P. & Weissman, J. S. (2004) *J. Cell Biol.* **164,** 341–346.
47. Tu, B. P. & Weissman, J. S. (2002) *Mol. Cell* **10,** 983–994.
48. Silva, J. P., Kohler, M., Graff, C., Oldfors, A., Magnuson, M. A., Berggren, P. O. & Larsson, N. G. (2000) *Nat. Genet.* **26,** 336–340.
49. Ristow, M., Mulder, H., Pomplun, D., Schulz, T. J., Muller-Schmehl, K., Krause, A., Fex, M., Puccio, H., Muller, J., Isken, F., *et al.* (2003) *J. Clin. Invest.* **112,** 527–534.